

Article

Optimization of Integrated Energy System Considering Electricity and Hydrogen Coordination in the Context of Carbon Trading

Xiaofeng Li ¹, Bing Wang ², Duoyu Pan ², Xiong Yu ², Yanling Che ², Qianye Lei ², Lijia Yang ², Baofeng Wang ³ and Hao Lu ^{1,*}

¹ Laboratory of Energy Carbon Neutrality, School of Electrical Engineering, Xinjiang University, Urumqi 830047, China

² PetroChina Xinjiang Sales Co., Ltd., Urumqi 830011, China; yx-pds@petrochina.com.cn (X.Y.)

³ Qingdao Oket Instrument Co., Ltd., Qingdao 266000, China

* Correspondence: luhao@xju.edu.cn

Abstract: In order to improve the consumption of renewable energy and reduce the carbon emissions of integrated energy systems (IESs), this paper proposes an optimal operation strategy for an integrated energy system considering the coordination of electricity and hydrogen in the context of carbon trading. The strategy makes full use of the traditional power-to-gas hydrogen production process and establishes a coupling model comprising cogeneration and carbon capture equipment, an electrolytic cell, a methane reactor, and a hydrogen fuel cell. Taking a minimum daily operating cost and minimal carbon emissions from the system as objective functions, a mixed-integer nonlinear optimal scheduling model is established. This paper designs examples based on MATLAB R2021b and uses the GUROBI solver to solve them. The results show that compared with the traditional two-stage operation process, the optimization method can reduce the daily operation cost of an IES by 26.01% and its carbon emissions by 90.32%. The results show that the operation mode of electro-hydrogen synergy can significantly reduce the carbon emissions of the system and realize a two-way flow of electro-hydrogen energy. At the same time, the addition of carbon capture equipment and the realization of carbon recycling prove the scheduling strategy's ability to achieve a low-carbon economy of the scheduling strategy.

Keywords: integrated energy system; hydrogen fuel cell; electrolytic hydrogen production; carbon capture system



Citation: Li, X.; Wang, B.; Pan, D.; Yu, X.; Che, Y.; Lei, Q.; Yang, L.; Wang, B.; Lu, H. Optimization of Integrated Energy System Considering Electricity and Hydrogen Coordination in the Context of Carbon Trading. *Processes* **2024**, *12*, 873. <https://doi.org/10.3390/pr12050873>

Academic Editor: Paola Ammendola

Received: 22 February 2024

Revised: 12 April 2024

Accepted: 18 April 2024

Published: 26 April 2024



Copyright: © 2024 by the authors. Licensee MDPI, Basel, Switzerland. This article is an open access article distributed under the terms and conditions of the Creative Commons Attribution (CC BY) license (<https://creativecommons.org/licenses/by/4.0/>).

1. Introduction

With the continuous rise in temperature leading to frequent extreme weather events, many parts of the world are facing problems such as insufficient power generation, resource depletion, and ecological environment degradation. Among them, energy activities are the largest sources of CO₂ greenhouse gas emissions, accounting for nearly 90% of China's total CO₂ emissions [1,2]. Most of this CO₂ comes from fossil fuel combustion, with the power industry contributing over 40%. At the same time, the energy demand is constantly increasing, but it is facing energy supply security issues such as energy reserve shortages and changes in the international energy market which have prompted the acceleration of the development and utilization of renewable energy. However, it is challenging to meet the ever-increasing need for new energy consumption while depending only on the power system [3].

As a result, creating an integrated energy system (IES) that relies mostly on renewable energy has emerged as a key strategy for addressing the energy issue and improving the environment. The cooperative operation of the power system with thermal, natural gas, and other systems to produce a multi-source coordinated and multi-energy complementary

system is an innovative approach to increasing the quantity of renewable energy used [4]. Multi-energy complementarity, the deep integration of physical data, and coordinated interactions between sources, networks, loads, and storage are important features of the IES [5]. It is conducive to improving the safety and reliability of the energy supply, reducing risk associated with the energy supply, and meeting the needs of multiple energy users. Among these factors, the optimal scheduling of the integrated energy system is the key to realizing the rational allocation and utilization of energy. At present, with the goal of reducing carbon emissions, research on the optimization of IESs has changed from traditional economic dispatch to low-carbon economic dispatch.

In the process of new energy utilization, unpredictability and anti-peak characteristics in photovoltaic and wind power generation can lead to a serious waste of wind and solar energy resources [6]. Power-to-gas (P2G) technology has received increasing attention and undergone rapid development in recent years as an important technology that effectively solves the problems of wind and solar curtailment while also supporting the increasing demand for natural gas loads. P2G devices use water and carbon dioxide to convert renewable energy that cannot be utilized and stored into methane [7] and utilize the existing mature natural gas system infrastructure as a huge energy storage facility to build a new bridge between the power system and the natural gas system, further linking their planning and operation [8]. The significance of stochastic and integrated planning for electricity and natural gas networks was examined and shown by Saldarriaga et al. [9]. Zhang et al. [10] proposed using power-to-gas equipment to convert surplus electrical energy into natural gas, greatly improving the absorption capacity of new energy. Zeng et al. [11] proposed an optimization model for the collaborative planning of power and natural gas systems. In an integrated energy system, optimal site selection and planning for P2G technology have been carried out to minimize investment and operating costs. Additionally, simulation instances were used to illustrate the usefulness of the suggested approach.

In terms of carbon reductions in energy systems, carbon capture and storage (CCS) is currently the most effective CO₂ reduction technology which is conducive to achieving low carbon emissions in the energy industry and has broad application prospects [12]. Carbon capture technology offers an effective way to address the problem of the power-to-gas (P2G) carbon raw material cost [13]. Based on the characteristics of both, using CO₂ obtained via carbon capture as raw material for the P2G synthesis of methane can not only efficiently lower the running expenses of the system but also boost the usage efficiency of the captured CO₂ [14]. Therefore, the coupling of a carbon capture system and power-to-gas equipment can effectively improve the low-carbon economic operation performance of an IES [15].

Many scholars have conducted related research on the coupling of CCS and P2G technology. Alizad et al. [16] examined CCS and P2G coupling as a whole, took the CO₂ captured by CCS as high-quality carbon raw material for the P2G process, and established a coordinated optimization model of CCS and P2G coupling. Zhang et al. [17] extended the coupling model of P2G and CCS to an IES including electricity, heat, and gas, establishing an economical and environmental scheduling model in the context of a high level of wind power penetration, and proposed the concept of the dynamic utilization of carbon and fugitive-free emissions. Using demand-side flexible load characteristics on the load side, Chen et al. [18] proposed a joint operating mode linked with combined heat and power generation (CHP), CCS, and P2G. The total operation effect of the integrated energy system under four operation modes was examined and compared against the backdrop of carbon trading. The economics and low carbon footprint of IESs have significantly improved.

Nevertheless, when modeling P2G technology, the majority of previous research solely took into account the conversion of energy into methane, ignoring the intermediate process of converting electricity into hydrogen. A favored option for large-scale integrated green development and the storage and use of solar energy and wind power is hydrogen [19]. The long-term storage capacity and high mass–energy density of hydrogen energy storage (HES) make it a promising new large-scale energy storage technology [20]. Taking into account the price of transporting and storing hydrogen, by combining an IES with renewable energy for

hydrogen production and placing hydrogen production on the energy side of the system, we can avoid the constraint of natural gas pipelines on the hydrogen blending ratio and reduce transportation costs to an amount equivalent to about half the production cost, producing more environmentally friendly and economical hydrogen and thereby further improving the competitiveness of hydrogen compared to fossil fuels [21].

Therefore, the synergistic interaction between electricity and hydrogen is an important direction of energy development. The process of coupling electricity and hydrogen includes electrolytic hydrogen production, methanation, and hydrogen power generation. Existing research indicates that the energy conversion efficiency of electrolysis for hydrogen production exceeds 80%, while the efficiency of methanation is less than 60% [22]. Due to the higher combustion efficiency of hydrogen, prioritizing the high-grade utilization of hydrogen in the electricity and hydrogen coupling process can improve the economic efficiency of IESs. A planning and optimization model for regional integrated energy systems that incorporates hydrogen and takes economic and environmental efficiency into account was developed by Wang et al. [23]. Li et al. [24] built a multi-microgrid system with hybrid energy storage consisting of PV cells, batteries, fuel cells, and electrolyzers. Varela et al. [25] considered the start–stop characteristics of electrolytic cells and introduced a 0–1 variable to represent the switching of operating states, establishing a mixed-integer linear model. At the same time, the electrolytic cell has variable load characteristics and can flexibly switch between overload, variable-load, and low-load states. Deng et al. [26] established a non-fixed-efficiency energy efficiency model by considering the non-linear relationship between the operating efficiency of equipment such as electrolytic cells and fuel cells and variations in input power. The above research focuses on the energy consumption process and the modeling of hydrogen in the operation of electricity–hydrogen coupling equipment. However, the impact of CCS, P2G technology, the combined operation of hydrogen fuel cells, and multi-energy network constraints on the low-carbon economy of the system is rarely considered.

Therefore, against the backdrop of carbon trading, this paper establishes a coupling optimization model for cogeneration and carbon capture equipment, P2G technology, and hydrogen fuel cells (HFCs) under various energy network constraints. Based on a MATLAB software design example, the minimum total operating cost and the lowest total carbon emissions of the system are taken as objective functions, and the GUROBI commercial solver is used to solve the problem. By comparing and analyzing the scheduling results of different operation strategies of the system, the effectiveness of the proposed operation strategy is verified.

The following are this article's primary contributions:

- (1) An optimal scheduling model of CHP, CCS, P2G, and HFC joint operation in a carbon-trading mode is constructed which improves the flexibility of converting energy between electricity, hydrogen, and gas.
- (2) Considering the synergy of electricity and hydrogen, the traditional P2G operation process is replaced by the coupled operation of an electrolytic cell, a methane reactor, and a hydrogen fuel cell, forming a two-way flow of energy between electricity and hydrogen which can give full play to the advantage of the high energy efficiency of hydrogen energy and reduce the cascade loss of energy.
- (3) The adjustable thermoelectric ratio of CHP to HFC is beneficial to thermoelectric decoupling and enhances the flexibility of the system's thermal–electric conversion.

2. The IES Operation Framework Considering CCS and Hydrogen Production in the Context of a Carbon Trading Mechanism

The low-carbon industrial park IES mentioned in this article, which takes into account CCS and electric hydrogen production, consists of an electrical subsystem, a thermal subsystem, and a gas subsystem. Figure 1 displays a structural diagram of the system. Photovoltaic (PV) units, a wind turbine (WT), combined heat and power, a hydrogen fuel cell, and an energy storage system (ESS) are the primary components of the power

subsystem. The gas subsystem mainly consists of P2G technology and a gas storage system (GSS). The thermal system includes a CHP unit, gas boilers (GBs), an HFC, and a thermal storage system (TSS). The coupling relationship between the carbon capture subsystem and the two-stage P2G operation process is shown in Figure 2. The dotted line represent the traditional P2G operation process, without considering the utilization of hydrogen energy in the process of electrolytic hydrogen production. The combined operation of the electrolytic cell (EL), methane reactor (MR), and HFC can realize the synergistic complementation of electricity and hydrogen. The hydrogen energy consumed by the MR is converted into CH₄ through the Sabatier reaction and supplied to the gas load and gas thermal power units; the HFC consumes hydrogen energy to generate electrical and thermal energy. In addition, to improve operational flexibility, hydrogen storage tanks (HSs) are installed to store hydrogen energy. At the same time, the system can trade with external electricity, heat, and gas networks.

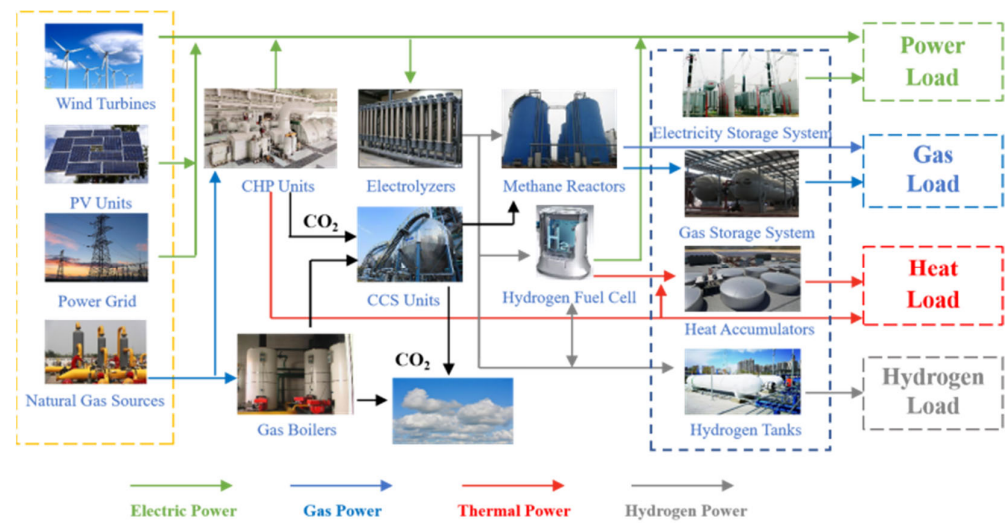


Figure 1. A structure diagram of the IES in the park.

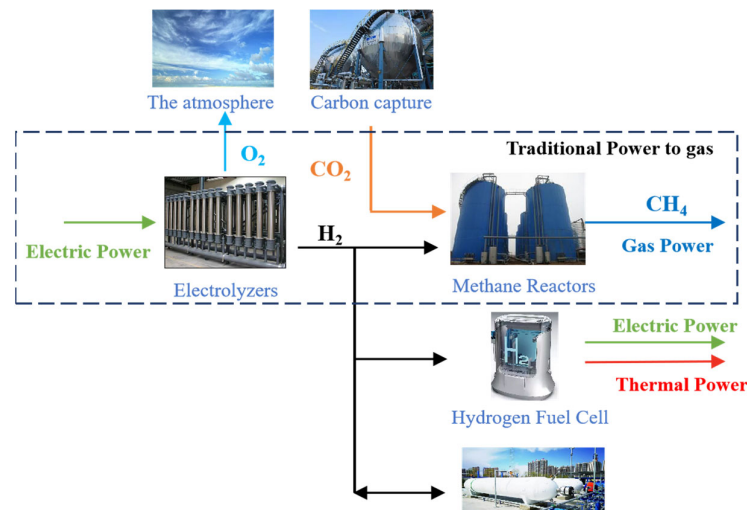


Figure 2. CCS coupling refines P2G.

2.1. IES Model Establishment

2.1.1. Combined Heat and Power Model (CHP)

The natural gas used in the CHP generators is burned to produce power. The waste heat boiler recovers the waste heat generated during the power generation process of the CHP to achieve cogeneration and the cascade utilization of energy [27]. This work

makes use of post-combustion capturing technologies. The carbon capture system sends the flue gas that is emitted from the CHP generating set to the absorption tower, where it is combined with a solvent. The mixture is then sent via the decomposition tower to produce compressed, high-purity CO₂, which is then provided to the P2G equipment. The power-to-gas apparatus converts the hydrogen and CO₂ produced by the electrolysis of water into methane (CH₄) using the electric energy of the bountiful renewable energy period. Formulae (1) through (5) explain how the CHP is coupled with the CCS and P2G equipment.

Its working model is as follows:

$$P_{\text{CHP},e}(t) = \eta_{\text{CHP},e} P_{\text{CHP},g}(t) \quad (1)$$

$$P_{\text{CHP},h}(t) = \eta_{\text{CHP},h} P_{\text{CHP},g}(t) \quad (2)$$

$$P_{\text{CHP},g}^{\min} \leq P_{\text{CHP},g} \leq P_{\text{CHP},g}^{\max} \quad (3)$$

$$-\varepsilon P_{\text{CHP},g}^{\max} \leq \Delta P_{\text{CHP},g}(t+1) - \Delta P_{\text{CHP},g}(t) \leq \varepsilon P_{\text{CHP},g}^{\max} \quad (4)$$

$$\alpha_{\text{CHP}}^{\min} \leq \frac{P_{\text{CHP},h}(t)}{P_{\text{CHP},e}(t)} \leq \alpha_{\text{CHP}}^{\max} \quad (5)$$

where $P_{\text{CHP},e}(t)$ denotes the power of the CHP system supplied to the IES, $P_{\text{CHP},g}(t)$ is the gas power input to the cogeneration system at a time t . $P_{\text{CHP},h}(t)$ is the heat energy output by the CHP system at a time t . The efficiency of the CHP system's conversion to electricity and heat is represented by the variables $\eta_{\text{CHP},e}$ and $\eta_{\text{CHP},h}$. ε is the climbing constraint coefficient. The natural gas input values at the CHP system's minimum and maximum powers are represented by $P_{\text{CHP},g}^{\min}$ and $P_{\text{CHP},g}^{\max}$, respectively. The thermoelectric ratio of the CHP has upper and lower bounds of $\alpha_{\text{CHP}}^{\max}$ and $\alpha_{\text{CHP}}^{\min}$, respectively.

2.1.2. Electrolyzer (EL)

The electrolyzer is the main electrical conversion device for the renewable-energy electrolysis of water to produce hydrogen. In this paper, an alkaline electrolytic cell is selected. The electric hydrogen production system uses electrolytic water to produce hydrogen and the hydrogen storage tank to store hydrogen under pressure when the power generation from wind and photovoltaic systems is greater than the load demand power. In case of insufficient wind and solar power generation, hydrogen fuel cells are used to convert hydrogen into electrical energy to supplement the power. The mathematical model is as follows:

$$P_{\text{EL},\text{H}_2}(t) = \eta_{\text{EL}} P_{\text{EL},e}(t) \quad (6)$$

$$P_{\text{EL},e}^{\min} \leq P_{\text{EL},e} \leq P_{\text{EL},e}^{\max} \quad (7)$$

$$-\varepsilon P_{\text{EL},e}^{\max} \leq \Delta P_{\text{EL},e}(t+1) - \Delta P_{\text{EL},e}(t) \leq \varepsilon P_{\text{EL},e}^{\max} \quad (8)$$

where $P_{\text{EL},e}(t)$ is the electric energy input into the EL, and $P_{\text{EL},\text{H}_2}(t)$ is the hydrogen energy generated by the EL. η_{EL} represents the EL's efficiency in converting energy, and its value is affected by voltage, current, and water quality. In order to simplify the model, the value in this paper is 0.87. $P_{\text{EL},e}^{\max}$ and $P_{\text{EL},e}^{\min}$ are the maximum and minimum electric power of the input EL, respectively.

2.1.3. Methane Reactor (MR)

The methanation reactor converts a certain proportion of mixed hydrogen and syngas (CO and CO₂) into methane through a catalytic exothermic reaction [28].

$$P_{\text{MR},g}(t) = \eta_{\text{MR}} P_{\text{MR},\text{H}_2}(t) \quad (9)$$

$$P_{\text{MR},\text{H}_2}^{\min} \leq P_{\text{MR},e} \leq P_{\text{MR},\text{H}_2}^{\max} \quad (10)$$

$$-\varepsilon P_{MR,H_2}^{\max} \leq \Delta P_{MR,H_2}(t+1) - \Delta P_{MR,H_2}(t) \leq \varepsilon P_{MR,H_2}^{\max} \quad (11)$$

where $P_{MR,H_2}(t)$ represents the hydrogen energy input to the MR, $P_{MR,g}(t)$ represents the natural gas power output by the MR, and η_{MR} represents the energy conversion efficiency of the MR. P_{MR,H_2}^{\min} and P_{MR,H_2}^{\max} represent the minimum and maximum values of the hydrogen energy input to the MR, respectively.

2.1.4. Hydrogen Fuel Cell (HFC)

Hydrogen fuel cells are important energy coupling devices for hydrogen energy utilization in multi-energy complementary systems which can realize the conversion between hydrogen energy and electric and thermal energy [29]. A direct supply of hydrogen energy to an HFC offers greater benefits since the amount of hydrogen energy converted from the HFC into electricity and heat energy is smaller than that which is transformed into methane through a methane reactor and then given to the CHP system or GB. This is because the efficiency of energy conversion is higher.

$$P_{HFC,e}(t) = \eta_{HFC,e} P_{HFC,H_2}(t) \quad (12)$$

$$P_{HFC,h}(t) = \eta_{HFC,h} P_{HFC,H_2}(t) \quad (13)$$

$$P_{HFC,H_2}^{\min} \leq P_{HFC,H_2} \leq P_{HFC,H_2}^{\max} \quad (14)$$

$$-\varepsilon P_{HFC,H_2}^{\max} \leq \Delta P_{HFC,H_2}(t+1) - \Delta P_{HFC,H_2}(t) \leq \varepsilon P_{HFC,H_2}^{\max} \quad (15)$$

$$\alpha_{HFC}^{\min} \leq \frac{P_{HFC,h}(t)}{P_{HFC,e}(t)} \leq \alpha_{HFC}^{\max} \quad (16)$$

where $P_{HFC,H_2}(t)$ is the hydrogen energy input into the HFC at a time t , and $P_{HFC,e}(t)$ and $P_{HFC,h}(t)$ are the electric and thermal energy output by the HFC at a time t . $\eta_{HFC,e}$ and $\eta_{HFC,h}$ are the conversion efficiencies of the HFC into electricity and heat, respectively. P_{HFC,H_2}^{\min} and P_{HFC,H_2}^{\max} are the maximum and minimum amounts of hydrogen power input to the HFC, respectively. α_{HFC}^{\min} and α_{HFC}^{\max} are the upper and lower limits of the thermoelectric ratio of the HFC.

2.1.5. Gas Boiler (GB)

When the CHP system and HPC cannot meet the IES's heat load demand, the remaining part can be provided by a GB. The gas boiler has strong adjustment flexibility and can be used independently, which can effectively improve the flexibility of the system's thermoelectric conversion.

$$P_{GB,h}(t) = \eta_{GB} P_{GB,g}(t) \quad (17)$$

$$P_{GB,g}^{\min} \leq P_{GB,g} \leq P_{GB,g}^{\max} \quad (18)$$

$$-\varepsilon P_{GB,g}^{\max} \leq \Delta P_{GB,g}(t+1) - \Delta P_{GB,g}(t) \leq \varepsilon P_{GB,g}^{\max} \quad (19)$$

where η_{GB} is the energy conversion efficiency of the GB, $P_{GB,g}(t)$ is the gas power input into the GB, and $P_{GB,h}(t)$ is the thermal power output by the GB at a time t . The maximum gas power input to the GB is denoted by $P_{GB,g}^{\max}$, and the minimum is denoted by $P_{GB,g}^{\min}$.

2.1.6. Energy Storage System (ESS)

Due to the similarity of energy storage equipment models such as electricity, heat, and gas models, this paper models the energy storage equipment such as electricity, heat, gas, hydrogen, etc., using a unified model, which is as described in Formulas (20)–(26).

$$P_{ES,i}(t) = P_{ESS,i}^{\text{cha}}(t) \eta_{ESS,i}^{\text{cha}} - \frac{P_{ESS,i}^{\text{dis}}(t)}{\eta_{ESS,i}^{\text{dis}}} \quad (20)$$

$$Q_i(1) = Q_i(T) \quad (21)$$

$$Q_i(t) = Q_i(t-1) + \frac{P_{ESS,i}(t)}{P_{ESS,i}^{\max}} \quad (22)$$

$$Q_i^{\min} \leq Q_i(t) \leq Q_i^{\max} \quad (23)$$

$$0 \leq P_{ESS,i}^{\text{cha}}(t) \leq X_{ESS,i}^{\text{cha}}(t)P_{ESS,i}^{\max}(t) \quad (24)$$

$$0 \leq P_{ESS,i}^{\text{dis}}(t) \leq X_{ESS,i}^{\text{dis}}(t)P_{ESS,i}^{\max}(t) \quad (25)$$

$$X_{ESS,i}^{\text{cha}}(t)X_{ESS,i}^{\text{dis}}(t) = 0 \quad (26)$$

where $P_{ES,i}(t)$ is the final output power of the energy storage device i at a time t , $P_{ESS,i}^{\text{cha}}(t)$ and $P_{ESS,i}^{\text{dis}}(t)$ are the charging and discharging power values of the type i energy storage device at a time t , respectively. $\eta_{ESS,i}^{\text{cha}}$, $\eta_{ESS,i}^{\text{dis}}$ are the charging and discharging efficiencies of the energy storage device i . $Q_i(t)$ is the capacity of the energy storage device i at a time t . $P_{ESS,i}^{\max}$ is the rated capacity of the energy storage device i . And i represents different types of energy storage modules. $X_{ESS,i}^{\text{cha}}(t)$ and $X_{ESS,i}^{\text{dis}}(t)$ are binary variables which represent the charge and discharge states of the energy storage device at a time t .

2.1.7. Carbon Capture System Model (CCS)

The carbon capture system directs the flue gas from the CHP generating set into the absorption tower. To create CO_2 with a higher degree of purity, the breakdown tower receives the flue gas, which is then combined with the solvent in the absorption tower [30]. The produced CO_2 is compressed and delivered to the MR. The MR produces methane (CH_4) from hydrogen and the CO_2 , which provides a gas source for the CHP system and gas boiler and realizes the recycling of carbon. The relationship between the amount of carbon captured and the power required for CCS is constrained by Equation (28). Formula (29) shows the maximum carbon capture constraint.

$$C_{\text{CCS}}(t) = \beta P_{\text{EL},e,\text{ccs}}(t) \quad (27)$$

$$P_{\text{CCS},e}(t) = \gamma C_{\text{CCS}}(t) \quad (28)$$

$$C_{\text{CCS}}(t) \leq \sum_{t=1}^T a_{\text{CO}_2} P'(t) + b_{\text{CO}_2} P'(t)^2 + c_{\text{CO}_2} \quad (29)$$

$$P'(t) = P_{\text{CHP},e}(t) + P_{\text{EL},e}(t) + P_{\text{CCS},e}(t) + \alpha_{\text{CHP}} P_{\text{CHP},h}(t) \quad (30)$$

where $C_{\text{CCS}}(t)$ is the amount of CO_2 required for the EL to consume a unit of power $P_{\text{EL},e,\text{ccs}}(t)$, $P_{\text{EL},e,\text{ccs}}(t)$ is the amount of electricity consumed by the hydrogen produced using electricity for the synthesis of methane, and $P_{\text{CCS},e}(t)$ is the power consumption of CCS at a time t .

2.2. IES Optimization Model in Carbon Trading Mode

In carbon trading, carbon emission rights are referred to as a commodity. The buyer pays the seller a certain sum of money in exchange for a specific number of carbon dioxide emissions, creating a carbon dioxide emission trade [31,32]. The trading system mainly exists to promote reductions in greenhouse gas (mainly carbon dioxide) emissions.

2.2.1. Carbon Emission Model

The carbon emission quota model C_{IES} is as follows:

$$C_{\text{IES}} = C_{\text{buy},e} + C_{\text{PV}} + C_{\text{Wind}} + C_{\text{CHP}} + C_{\text{GB}} \quad (31)$$

$$C_{\text{buy},e} = \delta_e \sum_{t=1}^T P_{\text{buy},e}(t) \quad (32)$$

$$C_{PV} = \delta_{PV} \sum_{t=1}^T P_{PV}(t) \quad (33)$$

$$C_{Wind} = \delta_{Wind} \sum_{t=1}^T P_{Wind}(t) \quad (34)$$

$$C_{CHP} = \delta_g \sum_{t=1}^T (P_{CHP,e}(t) + P_{CHP,h}(t)) \quad (35)$$

$$C_{GB} = \delta_{GB} \sum_{t=1}^T P_{GB,h}(t) \quad (36)$$

where $\delta_{e,PV,Wind,g,GB}$ is the carbon trading quota coefficient in kg/kWh.

The IES's actual carbon emission model C'_{IES} is as follows:

$$C'_{IES} = C'_{buy,e} + C'_{total} - C_{CCS} \quad (37)$$

$$C'_{buy,e} = \sum_{t=1}^T (a_1 + b_1 P_{buy,e}(t) + c_1 P_{buy,e}^2(t)) \quad (38)$$

$$C'_{total} = \sum_{t=1}^T (a_2 + b_2 P_{total}(t) + c_2 P_{total}^2(t)) \quad (39)$$

$$P_{total}(t) = P_{CHP,e}(t) + P_{CHP,h}(t) + P_{GB,h}(t) \quad (40)$$

where a_1, b_1, c_1 are the actual carbon emission calculation parameters corresponding to the purchased electricity, and a_2, b_2, c_2 are the calculation parameters of the carbon emission of the energy supply equipment consuming methane.

2.2.2. Total Cost of System Operation

The energy purchasing costs are as follows:

$$f_1 = \sum_{t=1}^T \alpha_e P_{buy,e}(t) + \sum_{t=1}^T \alpha_g P_{buy,g}(t) \quad (41)$$

where α_e represents the electricity price at a time t , and α_g represents the purchase price of natural gas at a time t .

Carbon transaction costs represent the benefits or expenditures of a system's carbon emissions in the carbon market. The carbon trading costs are as follows:

$$f_2 = \alpha_c (C'_{IES} - C_{IES}) \quad (42)$$

where α_c represents the carbon transaction cost coefficient.

The energy storage equipment operating costs are as follows:

$$f_3 = \alpha_i \sum_{t=1}^T P_{ESS,i}^{cha}(t) \eta_{ESS,i}^{cha} + \frac{P_{ESS,i}^{dis}(t)}{\eta_{ESS,i}^{dis}} \quad (43)$$

where α_i is the energy storage cost coefficient.

The punishment cost of abandoning wind and photovoltaic units is as follows:

$$f_4 = \sum_{t=1}^T \alpha_{PV} P_{PV,c}(t) + \sum_{t=1}^T \alpha_{Wind} P_{Wind,c}(t) \quad (44)$$

where α_{PV} and α_{Wind} are the penalty cost coefficients of abandoning photovoltaic and wind units, respectively.

3. Objective Functions and Constraint Conditions

3.1. Objective Function

The integrated energy system aims to minimize the intra-day economic dispatch cost F , and the objective function is as follows:

$$\min(F) = f_1 + f_2 + f_3 + f_4 \quad (45)$$

where F is the total cost of the IES operation. The IES takes the lowest daily operating cost as the objective function.

3.2. Constraint Conditions

3.2.1. Energy Balance Constraints

The power balance constraint is as follows:

$$P_{\text{buy},e} + P_{\text{PV}} + P_{\text{Wind}} + P_{\text{CHP},e} + P_{\text{HFC},e} + P_{\text{ESS},e}^{\text{dis}} = P_{\text{Load},e} + P_{\text{EL}} + P_{\text{CCS},e} + P_{\text{ESS},e}^{\text{cha}} \quad (46)$$

$$0 \leq P_{\text{buy},e} \leq P_{\text{buy},e}^{\text{max}} \quad (47)$$

The thermal power balance constraint is as follows:

$$P_{\text{CHP},h} + P_{\text{GB},h} + P_{\text{HFC},h} + P_{\text{ESS},h}^{\text{dis}} = P_{\text{Load},h} + P_{\text{ESS},h}^{\text{cha}} \quad (48)$$

The gas power balance constraint is as follows:

$$P_{\text{buy},g} + P_{\text{MR},g} + P_{\text{ESS},g}^{\text{dis}} = P_{\text{Load},g} + P_{\text{CHP},g} + P_{\text{GB},g} + P_{\text{ESS},g}^{\text{cha}} \quad (49)$$

$$0 \leq P_{\text{buy},g} \leq P_{\text{buy},g}^{\text{max}} \quad (50)$$

The hydrogen power balance constraint is as follows:

$$P_{\text{EL},\text{H}_2} + P_{\text{ESS},\text{H}_2}^{\text{dis}} = P_{\text{MR},\text{H}_2} + P_{\text{HFC},\text{H}_2} + P_{\text{ESS},\text{H}_2}^{\text{cha}} \quad (51)$$

The wind and solar output constraints are as follows:

$$0 \leq P_{\text{Wind}} \leq P_{\text{Wind}}^{\text{max}} \quad (52)$$

$$0 \leq P_{\text{PV}} \leq P_{\text{PV}}^{\text{max}} \quad (53)$$

3.2.2. Energy Storage Operation Constraint

The energy output of each device in the multi-source electric–heat–gas system is dependent on its individual equipment capacity. The power used for charging and draining the battery will have an impact on the procedure. The procedure of heat storage and release for the heat storage water tank will be influenced by the power of the heat storage and release process. Formulas (54)–(57) can be used to universally represent its limitation.

$$Q_{\text{ES},n,\text{min}}^t \leq Q_{\text{ES},n}^t \leq Q_{\text{ES},n,\text{max}}^t \quad (54)$$

$$0 \leq P_{\text{ES},n}^{\text{cha}} \leq P_{\text{ES},n,\text{max}}^{\text{cha}} \quad (55)$$

$$0 \leq P_{\text{ES},n}^{\text{dis}} \leq P_{\text{ES},n,\text{max}}^{\text{dis}} \quad (56)$$

$$P_{\text{ES},n}^{\text{cha}} P_{\text{ES},n}^{\text{dis}} = 0 \quad (57)$$

where $Q_{\text{ES},n,\text{max}}^t$ and $Q_{\text{ES},n,\text{min}}^t$ are the upper and lower limits of the energy storage capacity of type n . $P_{\text{ES},n,\text{max}}^{\text{cha}}$ and $P_{\text{ES},n,\text{max}}^{\text{dis}}$ are the maximum charging and discharging power values of the type n energy storage equipment, respectively.

4. Case Study

Basic Data

The IES-scheduling model constructed in this article contains multiple equality and inequality constraints. Due to the involvement of quadratic constraints, this problem is a mixed-integer nonlinear problem. The problem was solved using YALMIP 12.10.0, calling the GUROBI 11.0.0 commercial solver. This article selects an IES in a certain park as its research object, taking a 24 h optimization scheduling cycle of 1 day and a unit time of 1 h. Table 1 displays each piece of equipment's operational specifications and installation capacity.

Table 1. Model parameters.

Parameters	Values	Parameters	Values
$P_{CHP,g}^{min}$	0	$P_{CHP,g}^{max}$	600 kW
ϵ	0.2	α_{CHP}^{min}	0.5
α_{CHP}^{max}	2.1	η_{EL}	0.87
$P_{EL,e}^{min}$	0	$P_{EL,e}^{max}$	500 kW
P_{MR,H_2}^{min}	0	P_{MR,H_2}^{max}	250 kW
η_{MR}	0.6	P_{HFC,H_2}^{min}	0
P_{HFC,H_2}^{max}	250 kW	α_{HFC}^{min}	0.5
α_{HFC}^{max}	2.1	$\eta_{HFC,e}$	0.95
$P_{GB,g}^{min}$	0	$P_{GB,g}^{max}$	800 kW
η_{GB}	0.95	$P_{ESS,e}^{max}$	450 kW
$P_{ESS,h}^{max}$	500 kW	$P_{ESS,g}^{max}$	150 kW
P_{ESS,H_2}^{max}	200 kW	Q_e^{min}	45 kW
Q_e^{max}	405 kW	Q_h^{min}	50 kW
Q_h^{max}	450 kW	Q_g^{min}	15 kW
Q_g^{max}	135 kW	$Q_{H_2}^{min}$	20 kW
$Q_{H_2}^{max}$	180 kW	β	1.02 (kg/kWh)
γ	0.5 (kWh/kg)	a_{CO_2}	0.89 (kg/kWh)
b_{CO_2}	0.0017 (kg/kWh)	c_{CO_2}	26.15 (kg/kWh)
δ_e	0.728 (kg/kWh)	δ_{PV}	0.798 (kg/kWh)
δ_{Wind}	0.798 (kg/kWh)	δ_g	3.672 (kg/kWh)
δ_{GB}	3.672 (kg/kWh)	a_1	30 (kg/kWh)
b_1	−0.38 (kg/kWh)	c_1	0.0034 (kg/kWh)
a_2	3 (kg/kWh)	b_2	−0.004 (kg/kWh)
c_2	0.001 (kg/kWh)	α_c	53 (RMB/t)
α_e	0.1 (RMB/kWh)	α_h	0.04 (RMB/kWh)
α_g	0.5 (RMB/kWh)	α_{H_2}	1.4 (RMB/kWh)
α_{PV}	0.1 (RMB/kWh)	α_{Wind}	0.1 (RMB/kWh)
α_{PV}	0.1 (RMB/kWh)	α_{Wind}	0.1 (RMB/kWh)

In order to confirm whether the suggested low-carbon economic dispatch approach is effective, three different examples were set up for a verification analysis, as shown in Table 2. Case 1 does not consider electrical coupling, Case 2 considers traditional electric-to-gas coupling, and Case 3 considers the process of electricity-to-hydrogen conversion, taking into account the working characteristics of equipment such as electrolytic cells, methane reactors, and fuel cells, and finely modeling the energy consumption process and hydrogen energy equipment.

Figure 3 displays the park's demand curves for heating, gas, and electricity as well as the anticipated energy production from solar and wind power sources. In the area in which the system is situated, the price of natural gas is fixed at 0.35 CNY/(kW·h). Figure 4 illustrates the power grid's time-of-use electricity pricing.

Table 2. Case settings.

Cases	Conditions
Case 1	An IES without electric and gas coupling equipment.
Case 2	An IES with P2G in the traditional mode.
Case 3	An IES with an EL, MR, and HFC coupling operation.

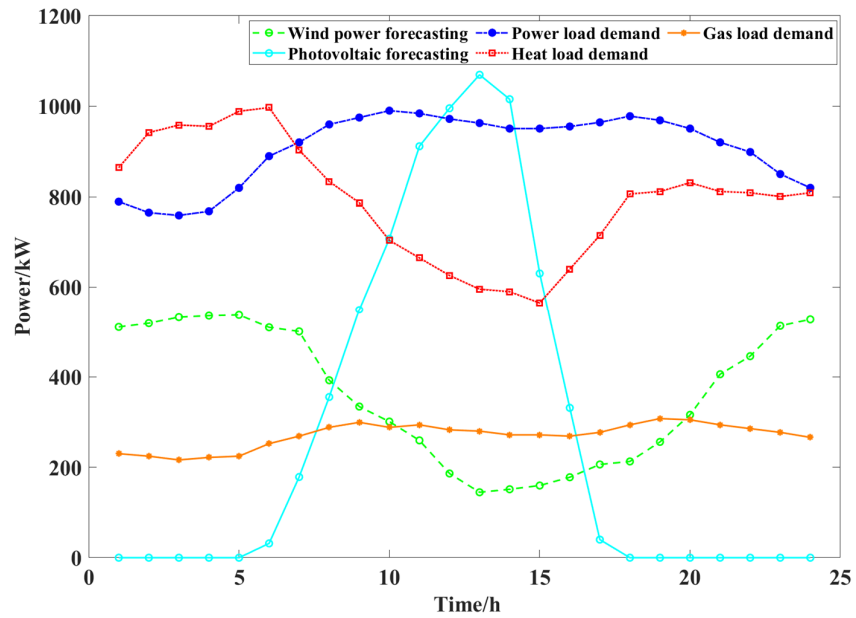


Figure 3. Renewable energy production forecast and load demand in park.

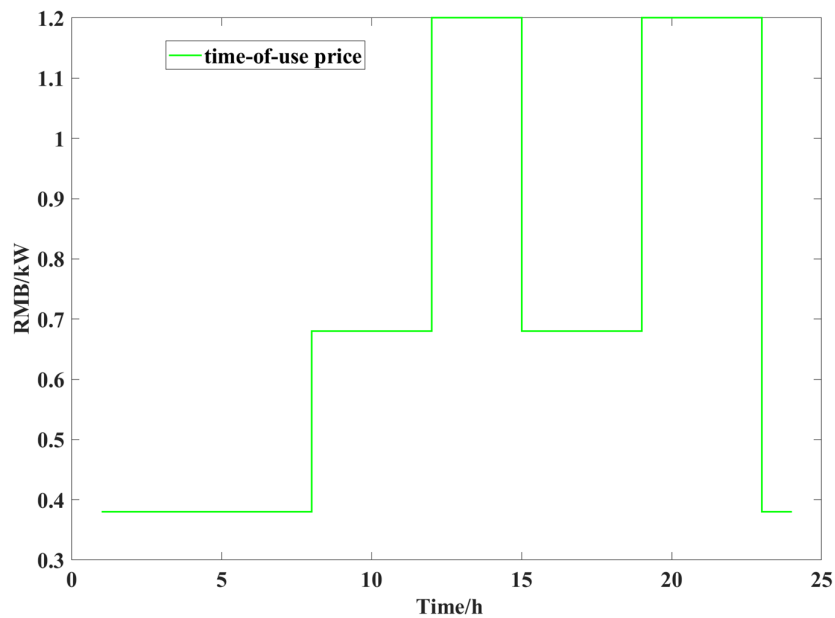


Figure 4. Electricity price setting.

Table 3 compares the optimization scheduling results for wind power and photovoltaic consumption, the CO₂ emissions, the carbon trading costs, and the daily operating costs of the system in three cases. The carbon emissions of each unit of the IES are analyzed for the three operating modes and shown in Table 4. Table 5 shows the specific composition of the operating cost of the system under the three operating conditions.

Table 3. Comparison of results.

Indices	Case 1	Case 2	Case 3
CO ₂ emissions (kg)	12,861.64	11,263.23	1426.41
Carbon transaction costs (RMB)	678.84	595.68	75.29
Wind power accommodation	92.34%	96.57%	100%
PV power accommodation	94.18%	96.16%	100%
Cost (RMB)	14,322.43	13,617.34	10,093.00

Table 4. Analysis of carbon emission subsystems.

Subsystems	Case 1	Case 2	Case 3
	CO ₂ (kg)	CO ₂ (kg)	CO ₂ (kg)
PV	−5128.70	−5229.80	−5377.50
Wind	−6351.90	−6650.10	−6808.60
CHP	+24,966.47	+23,975.09	+19,042.61
GB	−2206.97	−2175.86	−893.16
CCS		−186.23	−4055.33

Note: “+” means release CO₂; “−” means absorption CO₂ or carbon quota.

Table 5. Economic analysis.

Economic Analysis	Case 1	Case 2	Case 3
Carbon transaction costs (RMB)	−678.84	−595.68	−75.29
Gas purchasing cost (RMB)	−9418.13	−9065.70	−4818.70
Electricity purchasing cost (RMB)	−3259.04	−3384.70	−5032.71
Penalty Cost (RMB)	−1214.51	−446.29	0
Energy storage cost (RMB)	−119.84	−125.80	−166.30

Note: “+” means income; “−” means expenditure.

Case 1 does not consider electrical and gas coupling equipment, and the total operating cost of the system is CNY 14,322.43, with carbon dioxide emissions of 12,861.64 kg. Case 2 considers P2G devices in the traditional mode, without considering hydrogen energy utilization. The total operating cost of the system is CNY 13,617.34, and the carbon dioxide emissions are 11,263.23 kg. The total operating cost of the Case3 system is CNY 10,093.00, and the carbon dioxide emissions are 1426.41 kg. In Case 3, the utilization rate of wind and solar energy reached 100%. The IES first input the surplus wind power into EL equipment for hydrogen production, consuming all the photovoltaic and wind power.

Compared with Case 1, Case 2 reduces daily carbon emissions by 1598.41 kg, a decrease of 12.4%. The daily operating cost is decreased by CNY 705, a 5% decrease, and the utilization rate of wind and solar energy is also improved. Case 2 adds P2G equipment, which can convert excess electricity into methane during periods of surplus wind and solar power output, providing it for gas storage or load supply, improving the on-site consumption of surplus wind and solar power output. Moreover, by utilizing the originally abandoned wind and solar power, the costs of purchasing electricity from the power grid and gas grid has been reduced, and the economic cost has been further optimized. From this, it can be seen that considering electrical coupling can greatly constrain carbon emissions and achieve the goal of reducing emissions. Based on the combination of the time-of-use electricity price and gas price, it can be seen that the system aims to optimize economic operation. At each stage at which the gas price is lower than the electricity price, the system will purchase as much natural gas as possible and supply electricity to the electricity load through the CHP system, thereby reducing the total cost of purchasing energy.

Compared with Case 1, Case 3 reduces daily carbon emissions by 11,435.23 kg, a decrease of 88.90%; The daily operating cost decreases by CNY 4229.43 and 29.53%. Compared with Case 2, Case 3 reduces the daily operating cost of the IES by 25.88% and reduces carbon emissions by 87.33%. In Case 3, the IES inputs surplus wind and solar energy into EL

equipment for hydrogen production, consuming all wind and solar energy. Figure 5 shows the hydrogen energy balance diagram of Case 3, indicating that a portion of the hydrogen energy is transported to an HFC for thermoelectric production, while the other portion is transported to an MR for methane synthesis. Due to the fact that hydrogen energy is synthesized into methane through the MR and then transported to the GB and CHP system for energy supply, it will undergo multiple stages of energy loss. In the HFC, hydrogen energy is highly efficient in thermoelectric production while reducing an intermediate energy conversion link. Therefore, hydrogen energy is preferentially transported to the HFC for thermoelectric production, and the remaining hydrogen energy is then converted into methane through the MR, resulting in the highest energy utilization rate in Case 3.

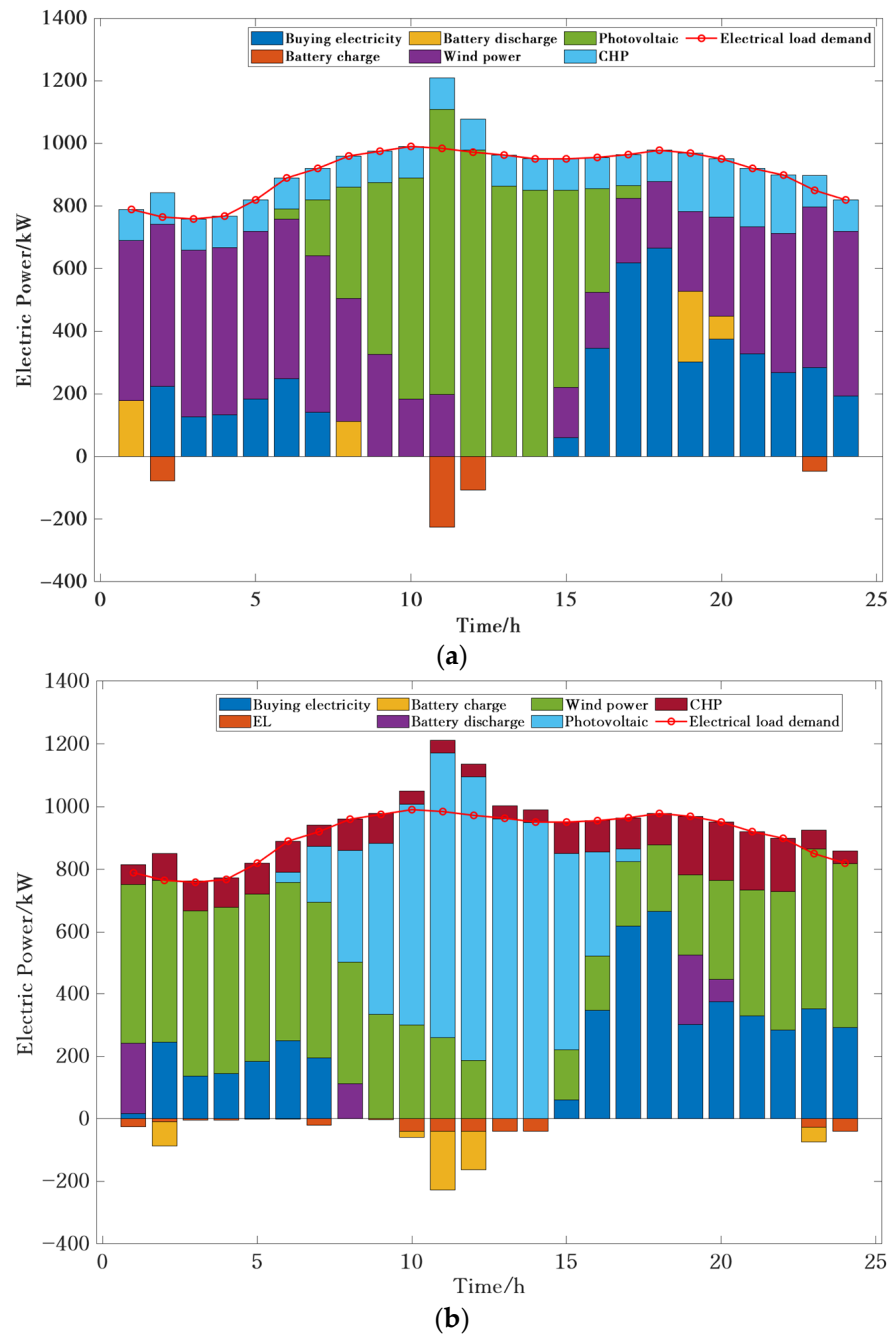


Figure 5. Cont.

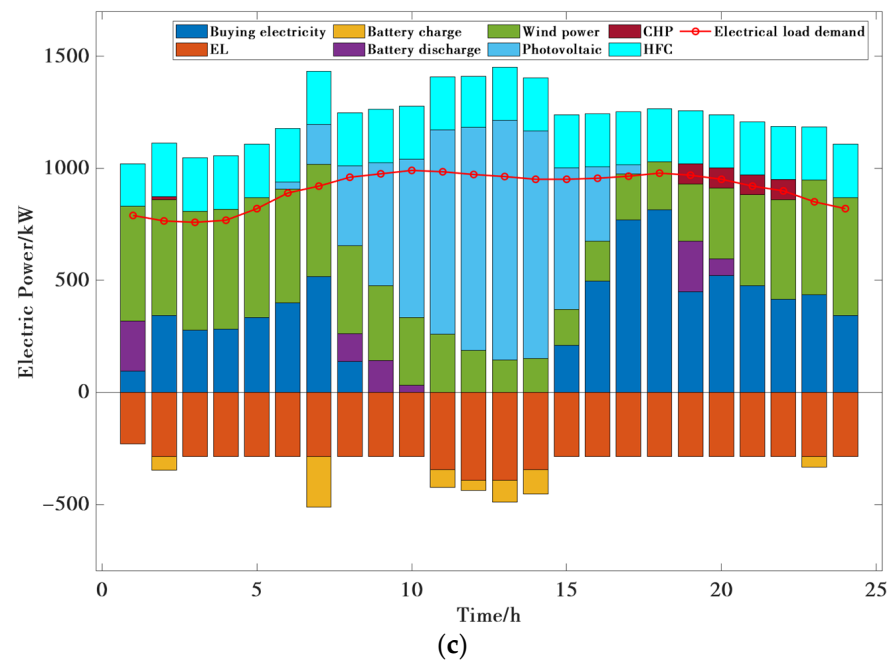


Figure 5. The electric power balance. (a) The electric power balance in Case 1; (b) the electric power balance in Case 2; (c) the electric power balance in Case 3.

In addition, compared with the optimization results of Chen et al. [33], because Case 3 considers a carbon capture subsystem (and the other conditions are the same), the actual carbon emissions of the system are greatly reduced by 92.75%. At the same time, the carbon purchase cost in the methanation process of the system is reduced, and the operating cost is reduced by 36.66%. Therefore, it can be proven that refining the process of converting electricity into hydrogen, considering the joint operation of electrolytic cells, methane reactors, fuel cells, and hydrogen storage tank equipment, can significantly reduce operating costs while reducing carbon emissions and has superior economic and environmental benefits. The optimization operation results have proven the effectiveness of the proposed optimization strategy.

Figures 5–7 show the hourly optimization scheduling results for Cases 1–3. The system preferentially uses renewable energy within the system, and the insufficiency is compensated by the external power grid and gas grid. Its scheduling aims to manage energy with the lowest daily operating cost and carbon emissions. Figure 5 shows the electrical power balance of the integrated energy system in different scenarios, reflecting the real-time power supply and demand and scheduling of the system. Case 2 and Case 3 add electric hydrogen production equipment and increase the consumption of new energy in periods of abundant wind and light resources. Figure 6 shows the thermal power balance of the IES in different scenarios. As shown in Figure 6, the trend of the thermal power curve is basically the same, but the response priority is different. In Case 3, due to the higher energy conversion efficiency of the HFC compared to the methane synthesis efficiency, the HFC has a higher energy priority. Figure 7 shows the balance of the IES's gas power in different cases involving the generation, consumption, and storage of methane. According to the actual demand and energy supply, the system reasonably arranges the production and utilization of gas, realizes a flexible allocation between electricity and gas, improves the efficiency of energy utilization, and reduces the operating cost of the system.

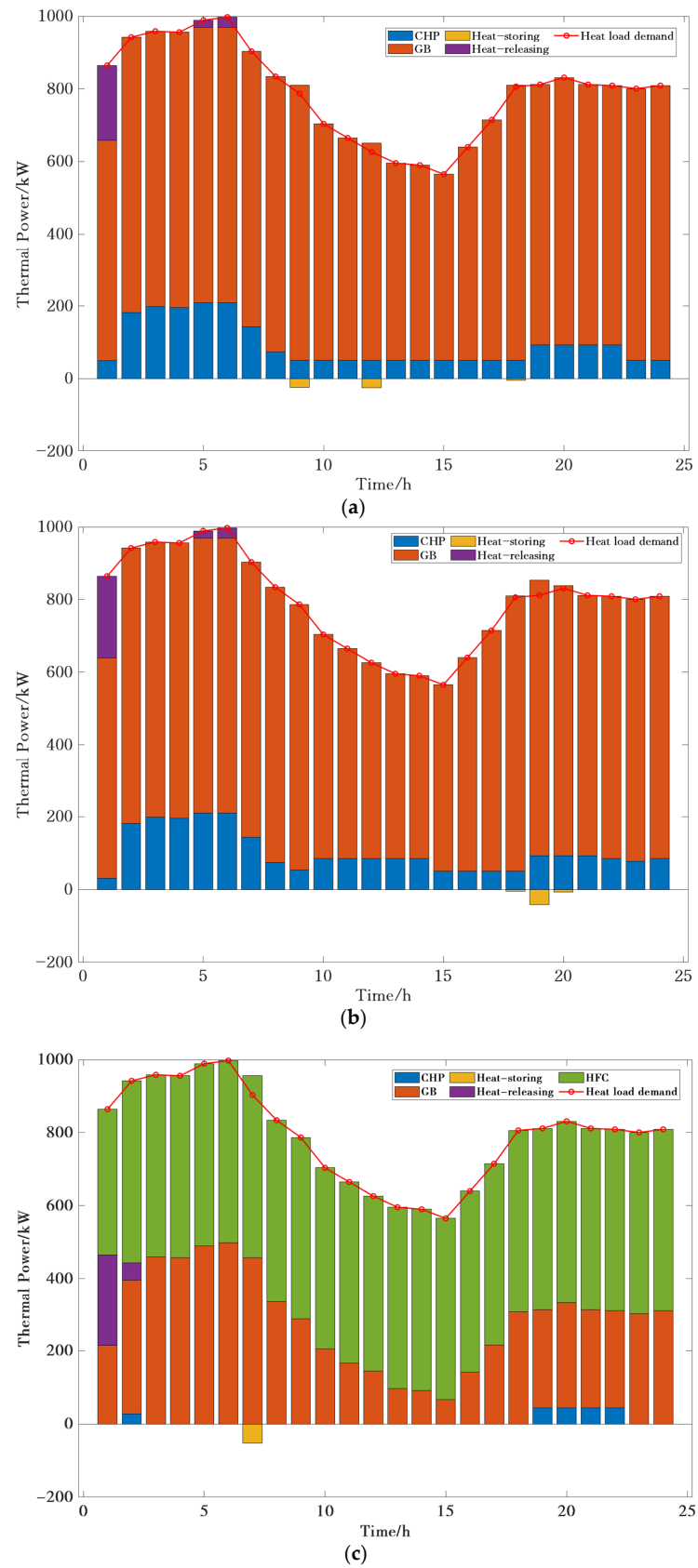


Figure 6. The heat power balance. (a) The heat power balance in Case 1; (b) the heat power balance in Case 2; (c) the heat power balance in Case 3.

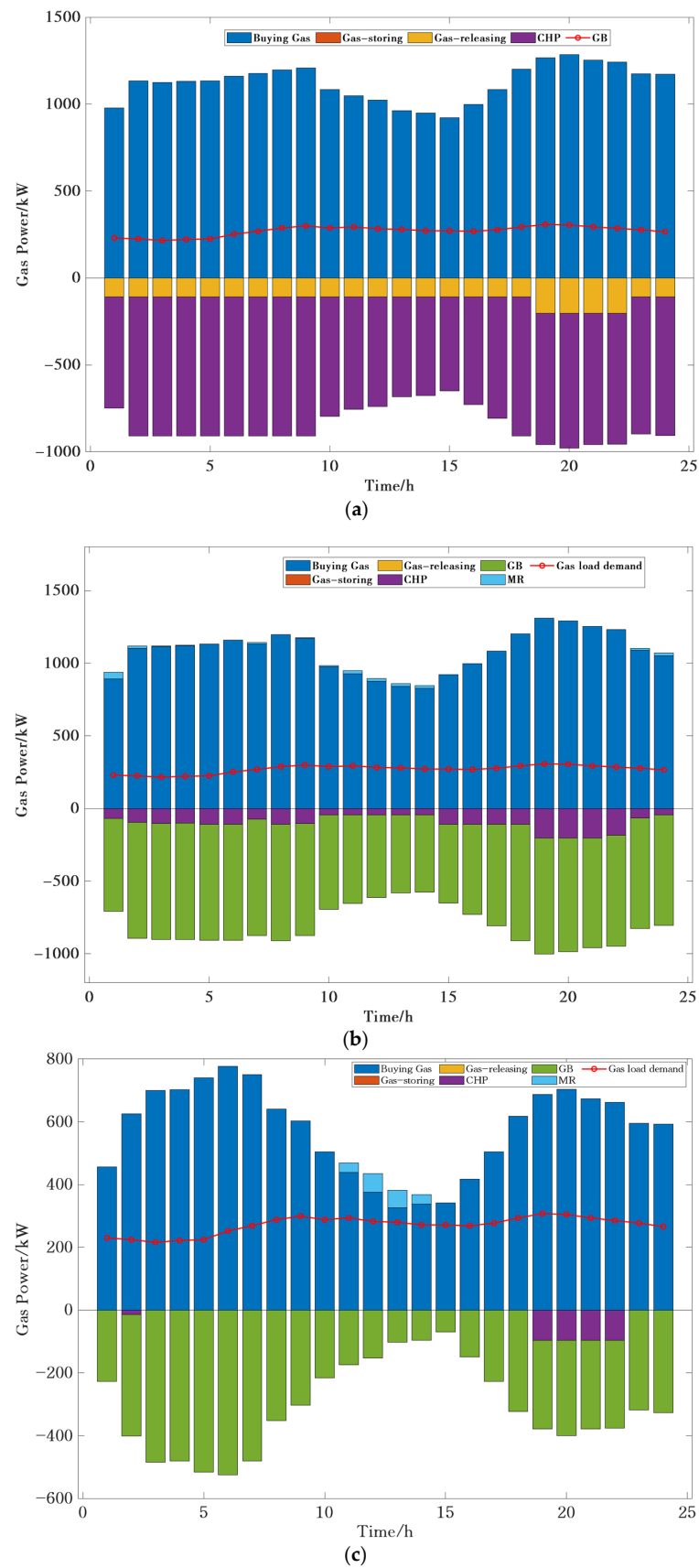


Figure 7. The gas power balance. (a) The gas power balance in Case 1; (b) the gas power balance in Case 2; (c) the gas power balance in Case 3.

Figure 8 shows the hydrogen power balance of the system in Case 3. In the period of 11:00–14:00, photovoltaic resources are very rich. The system effectively utilizes the photovoltaic power that exceeds the load demand and converts the excess electric energy into hydrogen energy via electrolytic hydrogen production, thereby reducing the abandoned power of the photovoltaic generator equipment.

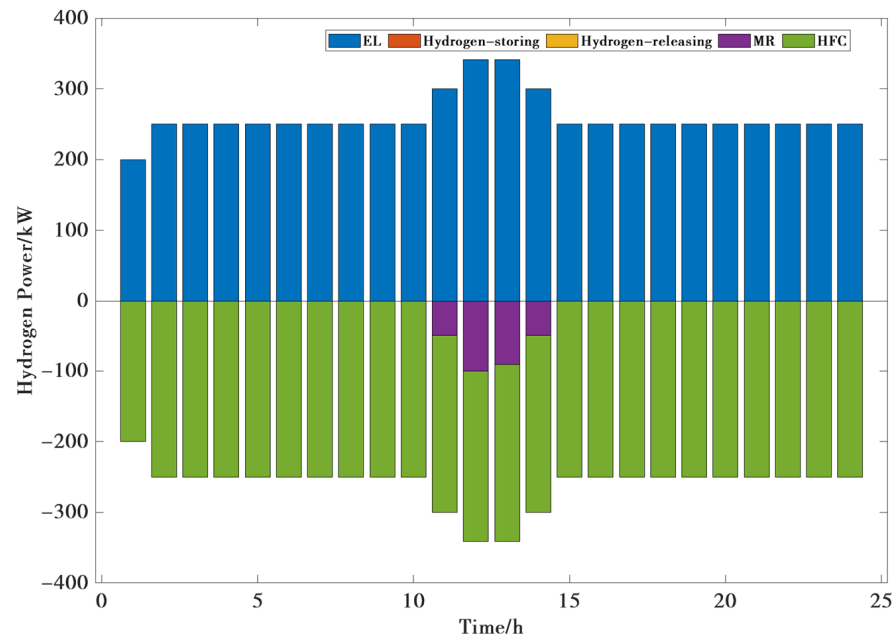


Figure 8. The hydrogen power balance in Case 3.

From an economic perspective, compared to Case 1, Case 3 has increased operating and maintenance costs due to the installation of EL, MR, HFC, and hydrogen storage tank equipment. To create hydrogen, however, the IES uses a surplus of electricity generated during the peak energy season. This can encourage the use of renewable energy sources and lower the prices of solar and wind waste. The combination of electric hydrogen production, carbon capture, and hydrogen fuel cells can yield a large reduction in carbon emissions which is economically feasible when taking into account the cost of carbon emissions and the gain in carbon value. In the meantime, future revenue from the sale of hydrogen could further boost the system's earnings due to the increasing capacity of the solar and wind energy units installed.

A strong link is seen between the system's CO₂ capture capacity and the electrolytic cell device's power consumption, as depicted in Figure 9. GB and the CHP system account for the majority of the IES's carbon emissions. Because methane synthesis and CCS have a strong carbon-hydrogen connection, the amount of carbon absorption power from CCS is dependent on the methane synthesis operating range. In order to achieve carbon recycling, the majority of the CO₂ released by the IES can be efficiently absorbed by the CCS and delivered to the MR for methane synthesis. At the same time, when renewable energy is plentiful, the electrolytic cell can utilize the abundant electricity for hydrogen production. Thus, taking into account the application of the "gas to heat" technique in the context of carbon trading can increase the methane synthesis system's working range, further minimize carbon emissions from the system, and completely realize the consumption and exploitation of new energy.

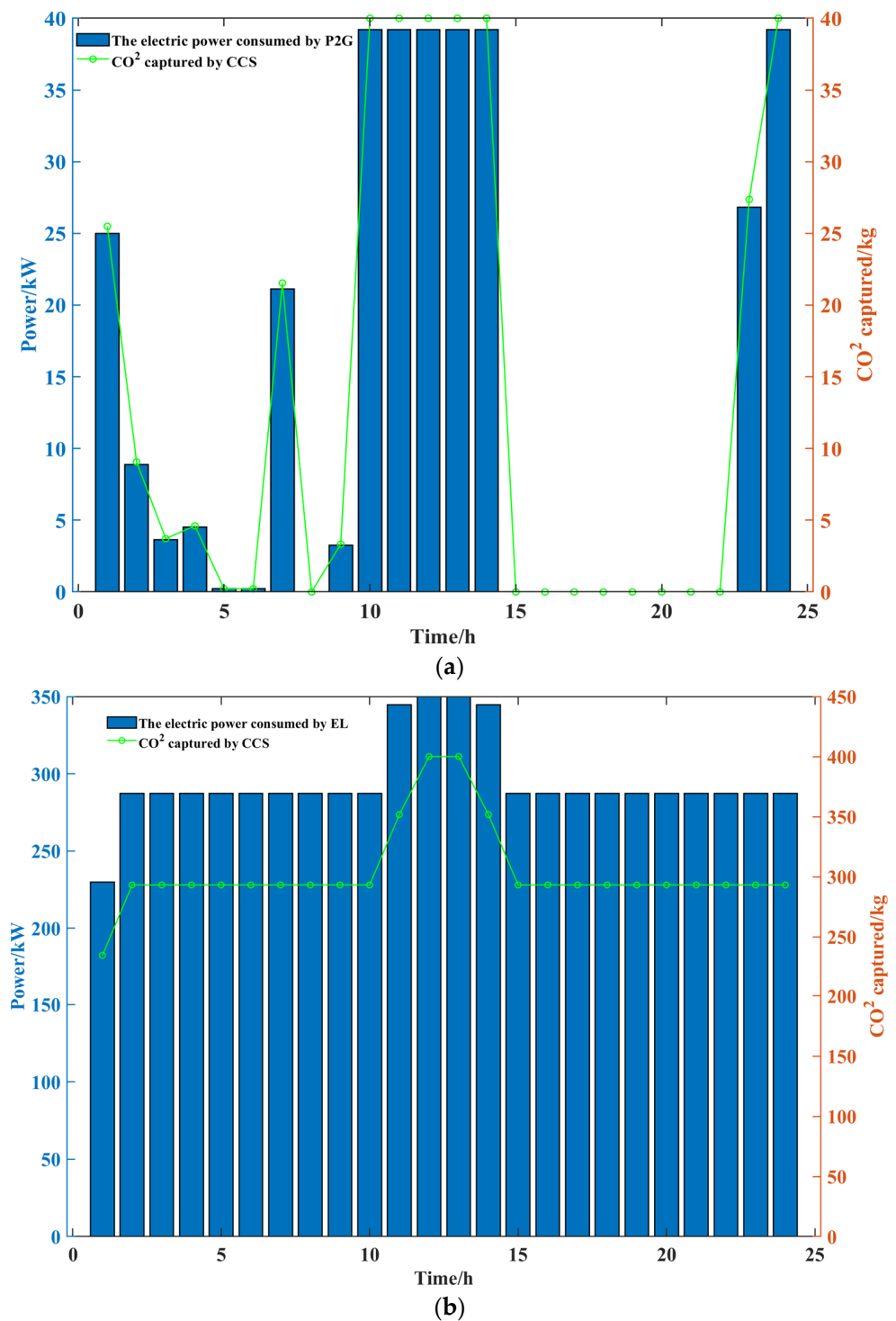


Figure 9. The coupling relationship between P2G and CCS in Case 2 and Case 3. (a) The coupling relationship between P2G and CCS in Case 2; (b) the coupling relationship between P2G and CCS in Case 3.

5. Conclusions

This work develops an optimal scheduling model for the joint operation of a CHP system, CCS, electric hydrogen production, and hydrogen fuel cells based on the carbon trading model in order to handle the difficulties of carbon reduction and new energy consumption. Based on validation studies using multiple scenarios, the following conclusions have been made:

- (1) CCS coupled with P2G technology can achieve CO₂ recycling and reduce gas purchases, effectively improving the low-carbon economic benefits of a system, reducing wind and light waste, and enhancing the renewable energy capacity of the IES.
- (2) By coupling the operation of an EL, MR and HFC, the synergy of electricity and hydrogen can be realized, which can give full play to the advantages of the high energy efficiency of hydrogen energy while promoting the consumption of wind power. Because the HFC can share part of the energy supply demand of the CHP system and GB, it can further reduce the carbon emissions of the system.
- (3) Considering the adjustable characteristics of the CHP system and HFC, according to the actual energy consumption, the output level of the CHP system and HFC can be adjusted in real time within an allowable range so as to realize the flexible conversion of heat and power and enhance the energy supply flexibility of the system.

In order to focus on the low-carbon goal and economy in the operation process of the system, this paper only considers the operation cost of the system and does not consider the economic cost of the system over its whole life cycle. It focuses on the supply-side operation strategy and does not consider demand-side scheduling. Demand-side scheduling can guide user energy consumption behavior and balance the supply and demand relationship of the system. Therefore, on the basis of this paper, the operation status of the IES with the participation of the demand-side response can be further analyzed in a follow-up study.

Author Contributions: Methodology, X.Y. and Q.L.; Software, Y.C.; Formal analysis, B.W. (Bing Wang); Investigation, D.P. and L.Y.; Data curation, X.Y.; Writing—original draft, X.L.; Supervision, H.L.; Project administration, B.W. (Baofeng Wang). All authors have read and agreed to the published version of the manuscript.

Funding: This research was funded by the National Key Research and Development Program of China (No. 2023YFB4102704), the National Natural Science Foundation of China (No. 52266017), and the Major Project of the National Social Science Foundation of China (No. 21&ZD133). This study was also supported by the Tianshan Talent Innovation Team Project of Xinjiang, the Xinjiang Natural Science Fund for Distinguished Young Scholars (No. 2021D01E08), the Xinjiang Regional Coordination Special Project—International Science and Technology Cooperation Program (No. 2022E01026), the Xinjiang Major Science and Technology Special Project (No. 2022A01002-2, No. 2022A01007-1, and No. 2023A01005-02), the Xinjiang Key Research and development Project (No. 2022B03028-2, No. 2022B01033-2, No. 2022B01022-1, and No. 2022B01020-4), the Central Guidance on Local Science and Technology Development Project (No. ZYYD2022C16), the Innovation Team Project of Xinjiang University (500122006021), and the High-Level Talents Project of Xinjiang University (No. 100521001).

Data Availability Statement: Data are contained within the article.

Conflicts of Interest: Authors Bing Wang, Duoyu Pan, Xiong Yu, Yanling Che, Qianye Lei, and Lijia Yang were employed by the company PetroChina Xinjiang Sales Co., Ltd., and author Baofeng Wang was employed by the company Qingdao Oket Instrument Co., Ltd. The remaining authors declare that the research was conducted in the absence of any commercial or financial relationships that could be construed as a potential conflict of interest.

References

1. Shan, Y.; Guan, D.; Liu, J.; Mi, Z.; Liu, Z.; Liu, J.; Schroeder, H.; Cai, B.; Chen, Y.; Shao, S.; et al. Methodology and applications of city level CO₂ emission accounts in China. *J. Clean. Prod.* **2017**, *161*, 1215–1225. [[CrossRef](#)]
2. Zheng, X.; Streimikiene, D.; Balezentis, T.; Mardani, A.; Cavallaro, F.; Liao, H. A review of greenhouse gas emission profiles, dynamics, and climate change mitigation efforts across the key climate change players. *J. Clean. Prod.* **2019**, *234*, 1113–1133. [[CrossRef](#)]
3. Ghaffour, N.; Bundschuh, J.; Mahmoudi, H.; Goosen, M.F.A. Renewable energy-driven desalination technologies: A comprehensive review on challenges and potential applications of integrated systems. *Desalination* **2015**, *356*, 94–114. [[CrossRef](#)]
4. Liu, L.; Zhai, R.; Xu, Y.; Hu, Y.; Liu, S.; Yang, L. Comprehensive sustainability assessment and multi-objective optimization of a novel renewable energy driven multi-energy supply system. *Appl. Therm. Eng.* **2024**, *236*, e121461. [[CrossRef](#)]

5. Dou, Z.; Zhang, C.; Wang, W.; Wang, D.; Zhang, Q.; Cai, Y.; Fan, R. Review on key technologies and typical applications of multi-station integrated energy systems. *Glob. Energy Interconnect.* **2022**, *5*, 309–327. [[CrossRef](#)]
6. Zhai, Z.; Gao, Y.; Luan, T.; Yan, R.; Dou, H.; Yu, Z.; Liu, Z. Multi-objective operation optimization analysis based on distributed energy sources. *J. Phys. Conf. Series.* **2023**, *2527*, 012010. [[CrossRef](#)]
7. Chen, Z.; Zhang, Y.; Ji, T.; Cai, Z.; Li, L.; Xu, Z. Coordinated optimal dispatch and market equilibrium of integrated electric power and natural gas networks with P2G embedded. *J. Mod. Power Syst. Clean Energy* **2017**, *6*, 495–508. [[CrossRef](#)]
8. Zheng, Q.; Qinglai, G.; Hongbin, S. Review of modeling, planning and operation of power-natural gas coupling system. *Glob. Energy Internet* **2020**, *3*, 14–26.
9. Saldarriaga-Cortés, C.; Salazar, H.; Moreno, R.; Jiménez-Estévez, G. Stochastic planning of electricity and gas networks: An asynchronous column generation approach. *Appl. Energy* **2018**, *233–234*, 1065–1077. [[CrossRef](#)]
10. Zhang, X.; Chan, K.; Wang, H.; Hu, J.; Zhou, B.; Zhang, Y.; Qiu, J. Game-theoretic planning for integrated energy system with independent participants considering ancillary services of power-to-gas stations. *Energy* **2019**, *176*, 249–264. [[CrossRef](#)]
11. Zeng, Q.; Fang, J.; Chen, Z.; Li, J.; Zhang, B. A multistage coordinative optimization for siting and sizing P2G plants in an integrated electricity and natural gas system. In Proceedings of the 2016 IEEE International Energy Conference (ENERGYCON), Leuven, Belgium, 3–7 April 2016; pp. 1–6.
12. Liu, E.; Lu, X.; Wang, D. A Systematic Review of Carbon Capture, Utilization and Storage: Status, Progress and Challenges. *Energies* **2023**, *16*, 2865. [[CrossRef](#)]
13. Ma, Y.; Wang, H.; Hong, F.; Yang, J.; Chen, Z.; Cui, H.; Feng, J. Modeling and optimization of combined heat and power with power-to-gas and carbon capture system in integrated energy system. *Energy* **2021**, *236*, 121392. [[CrossRef](#)]
14. Chen, M.; Lu, H.; Zheng, C. An integrated energy system optimization model coupled with power-to-gas and carbon capture. In Proceedings of the 2022 International Conference on Renewable Energies and Smart Technologies (REST), Tirana, Albania, 28–29 July 2022; Volume 1, pp. 1–5.
15. Mazza, A.; Bompard, E.; Chicco, G. Applications of power to gas technologies in emerging electrical systems. *Renew. Sustain. Energy Rev.* **2018**, *92*, 794–806. [[CrossRef](#)]
16. Alizad, E.; Rastegar, H.; Hasanzad, F. Dynamic planning of Power-to-Gas integrated energy hub considering demand response programs and future market conditions. *Int. J. Electr. Power Energy Syst.* **2022**, *143*, e108503. [[CrossRef](#)]
17. Zhang, X.; Zhang, Y. Environment-friendly and economical scheduling optimization for integrated energy system considering power-to-gas technology and carbon capture power plant. *J. Clean. Prod.* **2020**, *276*, 123348. [[CrossRef](#)]
18. Chen, M.; Lu, H.; Chang, X.; Liao, H. An optimization on an integrated energy system of combined heat and power, carbon capture system and power to gas by considering flexible load. *Energy* **2023**, *273*, e127203. [[CrossRef](#)]
19. Ren, Z.Y.; Luo, X.; Qin, H.L.; Jiang, Y.P.; Yang, Z.X. Mid/long-term optimal operation of regional integrated energy systems considering hydrogen physical characteristics. *Power Syst. Technol.* **2022**, *46*, 3324–3332.
20. Tao, Y.; Qiu, J.; Lai, S.; Zhao, J. Integrated Electricity and Hydrogen Energy Sharing in Coupled Energy Systems. *IEEE Trans. Smart Grid* **2020**, *12*, 1149–1162. [[CrossRef](#)]
21. Ozturk, M.; Dincer, I. Development of renewable energy system integrated with hydrogen and natural gas subsystems for cleaner combustion. *J. Nat. Gas Sci. Eng.* **2020**, *83*, 103583. [[CrossRef](#)]
22. Martinez-Frias, J.; Pham, A.-Q.; Aceves, S.M. A natural gas-assisted steam electrolyzer for high-efficiency production of hydrogen. *Int. J. Hydrogen Energy* **2003**, *28*, 483–490. [[CrossRef](#)]
23. Wang, Y.; Liu, C.; Qin, Y.; Wang, Y.; Dong, H.; Ma, Z.; Lin, Y. Synergistic planning of an integrated energy system containing hydrogen storage with the coupled use of electric-thermal energy. *Int. J. Hydrogen Energy* **2023**, *48*, 15154–15178. [[CrossRef](#)]
24. Li, Y.; Wang, R.; Zhao, Q.; Xue, Z. Technological advancement and industrialization path of Sinopec in carbon capture, utilization and storage, China. *Energy Geosci.* **2022**, *5*, 100107. [[CrossRef](#)]
25. Varela, C.; Mostafa, M.; Zondervan, E. Modeling alkaline water electrolysis for power-to-x applications: A scheduling approach. *Int. J. Hydrogen Energy* **2021**, *46*, 9303–9313. [[CrossRef](#)]
26. Deng, J.; Jiang, F.; Wang, W.; He, G.; Zhang, X.; Liu, K. Lowcarbon Optimized Operation of Integrated Energy System Considering Electric-heat Flexible Load and Hydrogen Energy Refined Modeling. *Power Syst. Technol.* **2022**, *46*, 1692–1704.
27. Oyedepo, S.O.; Fakeye, B.A. Waste heat recovery technologies: Pathway to sustainable energy development. *J. Therm. Eng.* **2021**, *7*, 324–348. [[CrossRef](#)]
28. Schaaf, T.; Grünig, J.; Schuster, M.R.; Rothenfluh, T.; Orth, A. Methanation of CO₂-storage of renewable energy in a gas distribution system. *Energy Sustain. Soc.* **2014**, *4*, 2. [[CrossRef](#)]
29. Li, Z.; Zhang, W.; Zhang, R.; Sun, H. Development of renewable energy multi-energy complementary hydrogen energy system (A Case Study in China): A review. *Energy Explor. Exploit.* **2020**, *38*, 2099–2127. [[CrossRef](#)]
30. Zhang, X.; Zhang, Y. Multi-objective optimization of integrated power-thermal-gas energy system at campus level with P2G and CCS. *Electr. Power Constr.* **2020**, *41*, 90–99.
31. Li, W.; Jia, Z. The impact of emission trading scheme and the ratio of free quota: A dynamic recursive CGE model in China. *Appl. Energy* **2016**, *174*, 1–14. [[CrossRef](#)]

32. Liu, L.; Chen, C.; Zhao, Y.; Zhao, E. China's carbon-emissions trading: Overview, challenges and future. *Renew. Sustain. Energy Rev.* **2015**, *49*, 254–266. [[CrossRef](#)]
33. Chen, J.; Hu, Z.; Chen, Y.; Chen, W. Thermoelectric optimization of integrated energy system considering stepwise carbon trading mechanism and electricity hydrogen production. *Electr. Power Autom. Equip.* **2021**, *41*, 48–55.

Disclaimer/Publisher's Note: The statements, opinions and data contained in all publications are solely those of the individual author(s) and contributor(s) and not of MDPI and/or the editor(s). MDPI and/or the editor(s) disclaim responsibility for any injury to people or property resulting from any ideas, methods, instructions or products referred to in the content.